Chapter 2
Thermal, Photophysical, and Photochemical Processes

A proper definition of *thermal* (photothermal) and *non-thermal* (photochemical) laser processing would require a detailed knowledge of the fundamental interactions between laser light and matter, and of the various relaxation times involved. This information is available only for a few special systems. For this reason, the definitions usually employed are not very strict. We shall consider a laser-induced process as thermally activated if the thermalization of the excitation energy is fast compared to both the excitation rate and the initial processing step. The term photochemical is used if the laser-induced process proceeds *mainly* non-thermally. If both thermal and non-thermal mechanisms are significant, we denote the process as *photophysical*. Particularly in connection with photo-decomposition processes, we frequently use, instead of photothermal and photochemical, the terms pyrolytic and photolytic, respectively.

If laser processing is thermally activated, the state of the system is described by the temperature and the total enthalpy. The latter is relevant only if phase changes or chemical reactions take place. For a quantitative analysis and optimization of a particular process, the laser-induced temperature distribution must be known. In laser-microchemical processing, direct temperature measurements have been performed with a reliable degree of accuracy in only a very few cases. Frequently, laser-induced temperatures can only be calculated. In fact, many features in thermal processing can be qualitatively, and in some cases even quantitatively, analyzed on this basis.

Photochemical laser processing is determined by the *selectivity* of the excitation. In a gas or liquid, the selectivity is characterized by the number density of (selectively) excited, ionized, or dissociated species. In a solid, the degree of selectivity is determined by the number density of non-equilibrium photoelectrons, electron–hole pairs, photodissociated bonds, etc.

2.1 Excitation Mechanisms, Relaxation Times

The *primary* interactions between light and matter are always non-thermal. In laser processing, the relevant excitations can be classified into those of the solid substrate to be processed, those of the ambient medium, and those of the adsorbate–adsorbent system.

D. Bäuerle, *Laser Processing and Chemistry,* 4th ed.,
DOI 10.1007/978-3-642-17613-5_2,

In solids, light can interact with elementary excitations that are optically active. Among those are different types of electronic excitations (inter- and intraband excitations, excitons, plasmons, etc.) and excitations of phonons, polaritons, magnons, etc. Additionally, there may be localized or non-localized electronic or vibrational states that are related to defects, impurities, or the solid surface itself. Some of these transitions are schematically shown in Fig. 2.1.1. The energy E_g describes the distance between the highest valence band and the lowest conduction band. In recent years, excitations of material surfaces/interfaces have gained increasing interest. Of particular importance in nanooptics are surface-plasmon polaritons (SPPs) excited at nanostructured metal/dielectric *interfaces* (Sect. 27.2.2). SPPs are surface electromagnetic waves that are coupled to (coherent) oscillations of conduction band electrons at the interface with a dielectric medium.

In liquids and gases, light can induce electronic, vibrational, and rotational transitions within single molecules.

If molecules or atoms become adsorbed on a solid surface, their electronic and vibrational properties change. As a consequence, one observes changes in absorption cross sections and selection rules for optical absorption, additional vibrational transitions, etc. Light can increase or decrease the density of adsorbed species,

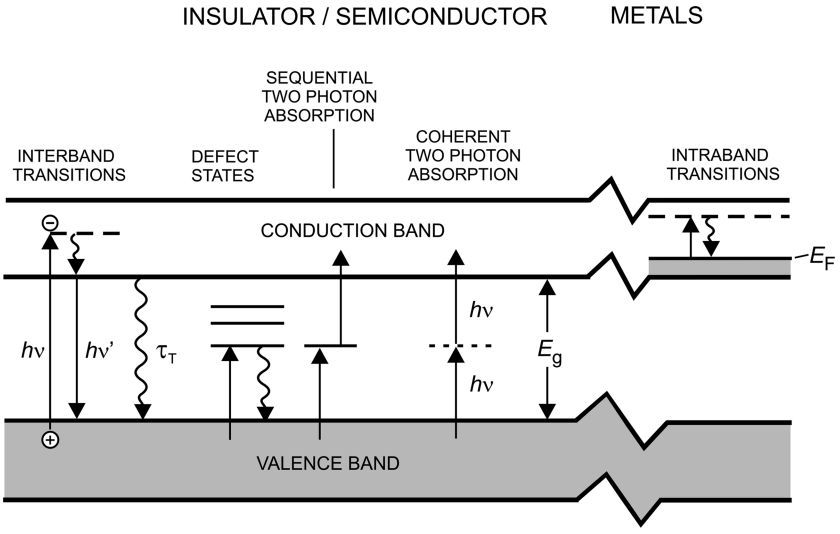

Fig. 2.1.1 Schematic of different types of electronic excitations in a solid. Only the highest valence band (VB) and the lowest conduction band (CB) are shown. *Straight lines* indicate absorption or emission of photons with different energies, $h\nu$. *Oscillating lines* indicate non-radiative processes. Interband transitions VB→CB take place if $h\nu \geq E_g$. In this process, electron–hole pairs are generated. Band-gap excitations are located in the near infrared (NIR) and visible (VIS) for semiconductors and in the ultraviolet (UV) for insulators. Defect, impurity and surface states often permit sub-bandgap excitations with $h\nu < E_g$. At high laser-light intensities, sequential multiphoton excitations via defect states or coherent multiphoton excitations become important. Intraband electronic transitions are typical for laser excitations in metals, and in semiconductors at elevated temperatures. E_F is the Fermi-energy

e.g., via excitations of the solid, the (free) gas- or liquid-phase molecules, or the adsorbate–adsorbent complex.

In all systems, different elementary excitations are coupled via anharmonic or higher order dipolar (multipolar) interactions.

High laser-light intensities allow high excitation densities to be generated, thermally or non-thermally. The density of excited molecules, atoms, ions, radicals, electrons, etc., can exceed 10^{22} species/cm^3. The coupling of elementary excitations among each other and with the intense laser radiation can cause a number of *new* phenomena. Prominent examples are changes in absorption cross sections, thermal runaway in metals and semiconductors, thermal self-focusing in transparent media (including the ambient medium), high densities of free carriers generated by interband excitation or impact ionization in semiconductors and insulators. With even higher laser-light intensities, *non-linear* optical phenomena such as self-focusing, multiphoton processes, etc., become important. With very high intensities, the formation of plasmas, shock waves, detonation waves, etc., is observed.

The time for the thermalization of the excitation energy depends on the type of material and the laser parameters.

In *metals*, light is almost exclusively absorbed by conduction band electrons within a skin layer of, typically, 10 nm (intraband transitions, Fig. 2.1.1). The time between electron–electron collisions, τ_e, is of the order of 10^{-14} to 10^{-12} s (10 fs to 1 ps). Electron-phonon relaxation times, τ_{e-ph}, are much longer, due to the big difference between electron and ion masses. Depending on the strength of electron-phonon coupling, one finds $10^{-12}\,\text{s} \leq \tau_{e-ph} \leq 10^{-10}\,\text{s}$. Similar relaxation times are found for quasi-free (conduction band) electrons in semiconductors like Si.

In *non-metals*, interband electronic excitations can last much longer, ranging from, typically, 10^{-12} to 10^{-6} s. Excitations of *localized* electronic states associated with defects, impurities or surfaces may have much longer lifetimes. Optically active phonons and localized vibrations in non-metals can be directly excited by IR light.

In single, isolated molecules, electronic excitations decay within 10^{-14} to 10^{-6} s. The lifetime of *low* excited vibrational levels is, typically, 10^{-3} s. With the (high) molecular densities employed in laser-chemical processing, energy randomization between molecules with vibrational mismatches $\leq k_B T$ occurs via collisions within, typically, 10^{-10} to 10^{-4} s.

It should be emphasized that with the *high* light intensities achieved with lasers, excitation and energy relaxation mechanisms can be significantly altered with respect to those relevant at low to medium intensities. For example, in polyatomic molecules highly excited vibrational states may have lifetimes of 10^{-13} to 10^{-11} s only.

2.1.1 Thermal Processes

The thermalization of the excitation energy shall be described by the relaxation time τ_T. For a thermal process $\tau_T \ll \tau_R$, where τ_R characterizes the initial processing step or the inverse excitation rate, depending on which is smaller. For some systems,

however, this condition must be modified. τ_R can be the time required for desorption of species from the surface, or, for structural rearrangements of atoms or molecules within the surface, the time which characterizes the *initial* step in a chemical reaction, etc.

Let us consider a simple example: Assume a reaction that is mediated by collisions of gas-phase molecules with a Si surface. The reaction probabilities for thermal and non-thermal processes shall be equal. The Si shall be irradiated by a picosecond laser pulse with $h\nu > E_g(\mathrm{Si})$ and an intensity that generates a carrier density, $N_c \approx 10^{22}\,/\mathrm{cm}^3$ near the surface. This carrier density decreases via Auger recombination to 1% within about 10^{-10} s (Sect. 2.4). Due to electron–phonon coupling, the recombination energy is dissipated into heat within, typically, 10^{-12} to 10^{-11} s. With a gas pressure of 100 mbar and a temperature of 300 K, the impingement rate onto the surface is some 10^{22} molecules/cm^2 s. The number of surface atoms is about 10^{14} atoms/cm^2. The time for the initial reaction step between a gas-phase molecule and a surface atom is then $\tau_R \geq 10^{-8}$ s, which is very long compared to $\tau_T \leq 10^{-10}$ s. Thus, the effect of laser radiation is purely thermal. In other words, if $\tau_T \ll \tau_R$ the detailed excitation mechanisms become irrelevant and the laser can be considered simply as a heat source.

In spite of their thermal character, laser-driven thermophysical and thermochemical processes may be quite different from those initiated by a conventional heat source. There are various reasons for this: The laser-induced temperature rise can be localized in space and time. Temperatures of more than 10^4 K can be induced in a *small* volume which is defined by the laser focus and the material parameters. With short high-intensity laser pulses, heating rates up to more than 10^{15} K/s can be achieved. With such heating rates, the chemical relaxation time may be slow in comparison, and the chemical reaction takes place far from equilibrium. Another possibility is the selective excitation of a particular species, e.g., in a gas mixture. Furthermore, laser heating may change the optical properties of the medium and thereby introduce non-linearities in the interaction process. As a consequence of these various mechanisms, novel chemical reaction pathways and reaction products, novel material microstructures and phases, novel surface morphologies, and novel evaporation characteristics may occur.

2.1.2 Photochemical Processes

The term photochemical (photolytic) laser processing is used if the overall thermalization of the excitation energy is slow, i.e., if $\tau_T \geq \tau_R$. This condition frequently holds for chemical reactions of excited molecules among themselves or with the substrate surface, for photoelectron transfer and subsequent chemisorption of species on solid surfaces, for photochemical desorption of species from surfaces, etc. If we consider the example discussed above, but assume that the molecules are already adsorbed on the Si surface, photocarriers can *directly* interact with the adsorbate and thereby initiate a reaction. In this case τ_R is the time for charge

transfer (Sect. 15.1). With purely photochemical processes, the temperature of the system remains (almost) unchanged under laser-light irradiation.

Due to the high excitation densities, laser photochemistry can be quite different from standard photochemistry using lamps.

2.1.3 Photophysical Processes

Thermal and photochemical processes can be considered as limiting cases of photophysical processes. We denote a process as photophysical if both thermal and non-thermal mechanisms *directly* contribute to the overall processing rate. The degree of thermal and non-thermal contributions depends on the relative yield of the respective reaction channels.

2.1.4 A Simple Model

The classification into thermal, photophysical, and photochemical processes is often quite complex. Consider the situation shown in Fig. 2.1.2. A and A^* shall characterize the system in the ground state and in the excited state, respectively. If we ignore spontaneous emission, non-radiative transitions $A^* \rightarrow A$ are described by the thermal relaxation time, τ_T. The characteristic times for the reaction of A and A^* with C are $\tau_A(T)$ and $\tau_{A^*}(T)$. It is often convenient to use, instead of relaxation times, τ_i, rate constants, $k_i \equiv k_i(T) = \tau_i^{-1}$. Let us consider *low* excitation rates where $\tau_T \leq h\nu/\sigma I$ (σ is the excitation cross section).

If $\tau_T \ll \tau_{A^*}$ and $\tau_A \ll \tau_{A^*}$ the excitation energy is immediately dissipated into heat and the reaction is thermally activated. The reaction rate is determined by k_A.

If $\tau_T > \tau_{A^*}$ and $\tau_{A^*} \ll \tau_A$ the process is mainly photochemically activated. The reaction takes place via excited species A^*.

If $\tau_T \ll \tau_A, \tau_{A^*}$ but $\tau_{A^*} \ll \tau_A$, or if all these times are comparable, both the 'thermal channel' and the 'photochemical channel' are important. We denote this process as photophysical. Let us study this situation in further detail and consider the kinetic equations

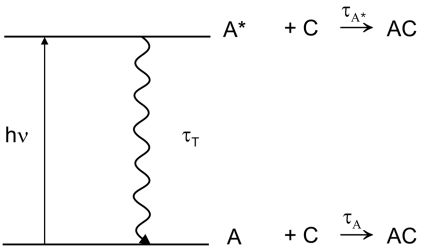

Fig. 2.1.2 A simple model for the competition between a thermal and a photochemical reaction. Stimulated emission is not indicated

$$\frac{\mathrm{d}N_\mathrm{A}}{\mathrm{d}t} = \frac{\sigma I}{h\nu}\,(N_{\mathrm{A}^*} - N_\mathrm{A}) + \frac{N_{\mathrm{A}^*}}{\tau_\mathrm{T}}\ ,$$
$$\frac{\mathrm{d}N_{\mathrm{A}^*}}{\mathrm{d}t} = \frac{\sigma I}{h\nu}\,(N_\mathrm{A} - N_{\mathrm{A}^*}) - \frac{N_{\mathrm{A}^*}}{\tau_\mathrm{T}}\ . \qquad (2.1.1)$$

Here, the reaction of A and A^* with C has been assumed to be so slow that the related changes in N_A and N_{A^*} can be ignored. The total density of species is then $N = N_\mathrm{A} + N_{\mathrm{A}^*}$ and quasi-stationary conditions are achieved after time $t \approx \tau_\mathrm{T}$. With $\mathrm{d}N_\mathrm{A}/\mathrm{d}t = \mathrm{d}N_{\mathrm{A}^*}/\mathrm{d}t = 0$, we obtain from (2.1.1) the quasi-stationary densities $\tilde{N}_\mathrm{A}$ and $\tilde{N}_{\mathrm{A}^*}$. The sum of reaction rates via the thermal channel, $W_\mathrm{T} \approx k_\mathrm{A}\tilde{N}_\mathrm{A}$, and the photochemical channel, $W_\mathrm{PC} \approx k_{\mathrm{A}^*}\tilde{N}_{\mathrm{A}^*}$, is then

$$W = W_\mathrm{T} + W_\mathrm{PC} = k_\mathrm{A}\tilde{N}_\mathrm{A}\left[1 + \frac{k_{\mathrm{A}^*}}{k_\mathrm{A}}\left(1 + \frac{h\nu}{\sigma I \tau_\mathrm{T}}\right)^{-1}\right]\ . \qquad (2.1.2)$$

The relative importance of the photochemical and thermal channels is determined by the second term in the parentheses. When the laser beam is switched off, the contribution of the photochemical channel decays within the characteristic time τ_T. Afterwards, the process is determined by k_A only.

This example shows, in a transparent way, how the competition between thermal and photochemical processes is determined by different time constants.

2.1.5 Chemical Relaxation

Let us consider a thermochemical process which is characterized by a chemical relaxation time, τ_ch, given by

$$\frac{1}{\tau_\mathrm{ch}} \equiv k_\mathrm{ch} = -\frac{1}{\Delta N_i}\frac{\mathrm{d}N_i}{\mathrm{d}t}\ , \qquad (2.1.3)$$

where N_i is the number density of species i, and ΔN_i its deviation from the equilibrium value. If the heating rate

$$\frac{1}{\tau_\mathrm{t}} \equiv k_\mathrm{t} = \frac{1}{T}\frac{\mathrm{d}T}{\mathrm{d}t} \qquad (2.1.4)$$

is small compared to k_ch, the system is in chemical equilibrium. If, on the other hand, $k_\mathrm{t} \gg k_\mathrm{ch}$, the system is far from equilibrium. This is the regime of non-equilibrium thermochemistry where novel reaction pathways and reaction products may be observed. The situation is analogous to the case of fast cooling (quenching) of systems. In this case, a non-equilibrium chemical state can be frozen.

Non-equilibrium chemistry is important in laser-induced surface modification, alloying, synthesis, etc. Quenching of non-equilibrium states is also important with structural transformations where no chemical reactions take place (Chap. 23).

2.2 The Heat Equation

Temperature distributions induced by the absorption of laser radiation within gases, liquids, and solids have been calculated on the basis of the heat equation. In the most general case, the temperature $T \equiv T(\boldsymbol{x}, t) = T(x_\alpha, t)$ is a function of both the spatial coordinates, x_α, and the time, t. With fixed laser parameters the temperature distribution depends on the optical absorption within the irradiated zone, on the transport of heat out of this zone and, if relevant, on transformation enthalpies for crystallization, melting and vaporization, chemical reaction enthalpies (exothermal or endothermal), etc. In the absence of heat transport by convection and thermal radiation, the heat equation can be written, in a coordinate system that is fixed with the laser beam, as

$$\varrho(T)c_\mathrm{p}(T)\frac{\partial T(\boldsymbol{x}, t)}{\partial t} - \nabla[\kappa(T)\nabla T(\boldsymbol{x}, t)] + \varrho(T)c_\mathrm{p}(T)\boldsymbol{v}_\mathrm{s}\nabla T(\boldsymbol{x}, t) = Q(\boldsymbol{x}, t) \; , \tag{2.2.1}$$

where $\varrho(T)$ is the mass density and $c_\mathrm{p}(T)$ the specific heat at constant pressure. $\boldsymbol{v}_\mathrm{s}$ is the velocity of the substrate (medium) relative to the heat source, Q (W/cm^3) (here, the substrate moves with a velocity $\boldsymbol{v}_\mathrm{s}$ whose direction is opposite to that shown in Fig. 6.1.1). If the substrate (workpiece) is uniform and isotropic, its thermal properties are characterized by a single thermal conductivity, κ, and a single heat diffusivity, D, which are related by

$$D = \frac{\kappa}{\varrho c_\mathrm{p}} \; . \tag{2.2.2}$$

If all temperature dependences in material parameters are ignored, the heat equation becomes linear. Values of ϱ, c_p, κ, and D are listed for various materials in Table II.

2.2.1 The Source Term

Subsequently, we assume that the light energy absorbed within the medium is totally transformed into heat. The source term can then be written as

$$Q(\boldsymbol{x}, t) = -\nabla \langle \boldsymbol{S} \rangle + U(\boldsymbol{x}, t) \; . \tag{2.2.3}$$

The function $U(\boldsymbol{x}, t)$ shall describe the additional energy per unit volume and time that is required or provided if phase changes or chemical reactions take place. $\langle \boldsymbol{S} \rangle = c\langle \boldsymbol{E} \times \boldsymbol{H} \rangle / 4\pi = I\hat{\boldsymbol{k}}_\ell$ is the time average of the Poynting vector. $\hat{\boldsymbol{k}}_\ell$ is a unit vector in the direction of the propagating light. This general expression for $\langle \boldsymbol{S} \rangle$ should be used if interference phenomena, optical inhomogeneities in the material, etc., must be considered. The propagation of light is characterized by the dielectric and magnetic permittivities of the medium, $\varepsilon = \varepsilon' + \mathrm{i}\varepsilon''$ and $\mu = \mu' + \mathrm{i}\mu''$. Henceforth,

we set $\mu' = 1$ and $\mu'' = 0$. The complex index of refraction can then be written as $\tilde{n} = \varepsilon^{1/2} = n + \mathrm{i}\kappa_\mathrm{a} \equiv n(1 + \mathrm{i}\kappa_0)$. Frequently, only the real part, n, is termed the refractive index. $\kappa_\mathrm{a} = n\kappa_0$ is the absorption index, and κ_0 the attenuation index. In the case of weak absorption and $\varepsilon'' \ll \varepsilon'$ we have $n \approx \varepsilon'^{1/2}$ and $\kappa_\mathrm{a} \approx \varepsilon''/2\varepsilon'^{1/2}$. In the low-density approximation which holds, for example, for dilute gases, $n - 1 \approx [\varepsilon' - 1]/2$ and $\kappa_\mathrm{a} \approx \varepsilon''/2$.

For monochromatic light and an isotropic medium, the first term in (2.2.3) can be written as

$$-\nabla \langle \boldsymbol{S} \rangle = \frac{\omega}{8\pi} \varepsilon'' |E_0|^2 \ ,$$

where $E(\boldsymbol{x}, t) = [E_0(\boldsymbol{x}) \exp(-\mathrm{i}\omega t) + \text{c.c.}]/2$ is the electric field. In the approximation of a (single) plane-wave and low absorption we obtain

$$\langle \boldsymbol{S} \rangle = \frac{c}{8\pi} n |E_0|^2 \hat{\boldsymbol{k}}_\ell = I \hat{\boldsymbol{k}}_\ell \ .$$

If we assume that the laser beam propagates in the z-direction, these two expressions yield the Bouguer–Lambert–Beer law,[1]

$$\frac{\mathrm{d}I(z)}{\mathrm{d}z} = -\alpha I(z) \ , \tag{2.2.4}$$

where

$$\alpha = \frac{4\pi\kappa_\mathrm{a}}{\lambda} = \frac{2\omega\kappa_\mathrm{a}}{c} = \frac{4\pi n\kappa_0}{\lambda} \tag{2.2.5}$$

is the (linear) absorption coefficient. λ is the wavelength in a vacuum. Values of α are listed for different materials in Table III. Instead of α, we often introduce the optical penetration depth, $l_\alpha = \alpha^{-1}$. The absorbed energy per unit volume and time is αI.

If the attenuation of the laser radiation is not solely caused by absorption but also by scattering, described by α_s, we have to replace α in (2.2.4) by the extinction coefficient, $\beta = \alpha + \alpha_\mathrm{s}$.

In a strict sense, Beer's law can be applied only if ε is uniform in space. Nevertheless, (2.2.4) is often also employed in photothermal processing, where the refractive index is *not* constant. Then, α is simply replaced by $\alpha = \alpha(T)$. Furthermore, for a tightly focused laser beam, the plane-wave approximation holds only within the Rayleigh length, z_R (Chap. 5).

---

[1] Throughout the literature, (2.2.4) is often termed the Lambert–Beer law or simply Beer's law; it was first derived experimentally in its integral form by *P. Bouguer* (1729), and theoretically by *I. G. Lambert* (1760). A mesoscopic interpretation of α was first given by *A. Beer* (1852).

2.2.2 Dimensionality of Heat Flow

An important quantity in thermal processing is the heat diffusion length,

$$l_{\mathrm{T}} \approx \zeta (D\tau_\ell)^{1/2} \; . \tag{2.2.6}$$

In *most* cases of transient heating that are characterized by a laser-beam dwell time, τ_ℓ, we choose $\zeta = 2$. This definition describes the $1/\mathrm{e}$ (spatial) decay in the temperature distribution

$$T(\boldsymbol{x}, t) \approx \frac{Q}{\varrho c_{\mathrm{p}} (4\pi Dt)^{m/2}} \exp\left(-\frac{|\boldsymbol{x}|^2}{4Dt}\right) \; , \tag{2.2.7}$$

which is a (fundamental) solution of the linear heat equation for a *point source* in infinite space,

$$\frac{\partial T}{\partial t} = D\nabla^2 T + \frac{Q}{\varrho c_{\mathrm{p}}} \delta(\boldsymbol{x}, t) \; .$$

The number m characterizes the (spatial) dimensionality of the problem, i.e., $m = 1, 2, 3$. Q is the total energy release and ϱ the density in $(\mathrm{g/cm^m})$.

It must be emphasized, however, that in all other cases the characteristic length, l'_{T}, which defines $T(l'_{\mathrm{T}}, t)/T(0, t) = 1/\mathrm{e}$, depends on the particular boundary-value problem under consideration and may differ significantly from (2.2.6).

The *dimensionality* of the heat flow is characterized by the relative size of l_{T} and other characteristic quantities such as the radius of the laser beam, w, the optical penetration depth, l_α, the thickness of the substrate, h_{s}, etc. If, for example, $l_{\mathrm{T}} \gg w, l_\alpha$, one has to consider the propagation of heat in three dimensions. On the other hand, for moderate absorption with $l_\alpha \leq l_{\mathrm{T}}$ and $l_{\mathrm{T}} \ll w$, lateral heat flow can be ignored and the temperature distribution in z-direction is obtained from the one-dimensional heat equation.

2.2.3 Kirchhoff and Crank Transforms

If the irradiated medium is isotropic, the temperature dependence of the thermal conductivity, $\kappa(T)$, can be eliminated from the heat equation by performing the Kirchhoff transform,

$$\theta(T) = \int_{T(\infty)}^{T} \frac{\kappa(T')}{\kappa(T(\infty))} \, \mathrm{d}T' \; , \tag{2.2.8}$$

where θ is a linearized temperature, and $T(\infty)$ the temperature at infinity, i.e., far away from the processed region. If κ is independent of temperature, the linearized

temperature is equal to the temperature rise, i.e., $\theta = \Delta T$. In terms of θ, the heat equation (2.2.1) has the form

$$\frac{1}{D(T(\theta))}\frac{\partial\theta}{\partial t} - \nabla^2\theta + \frac{\boldsymbol{v}_\mathrm{s}}{D(T(\theta))}\nabla\theta = \frac{Q}{\kappa(T(\infty))} \; . \tag{2.2.9}$$

An analytical solution of (2.2.9) is possible only in special cases. For an arbitrary geometry and temperature-dependent parameters D, α, and the reflectivity, R, only numerical solutions can be found.

With similar types of equations where D depends on time only, i.e. $D = D(t)$, and where $\boldsymbol{v}_\mathrm{s} = 0$ (see, e.g., Sect. 24.1), the Crank transform,

$$\tau = \int_0^t D(t')\,\mathrm{d}t' \; , \tag{2.2.10}$$

yields the linear equation

$$\frac{\partial\theta}{\partial\tau} - \nabla^2\theta = \frac{Q}{\kappa(T(\infty))} \; , \tag{2.2.11}$$

which can be solved analytically in many cases.

2.2.4 Phase Changes

If the laser power exceeds the threshold power for surface melting and evaporation, the temperature distribution can be calculated from the heat equation only when the latent heats of melting, ΔH_m, and evaporation, ΔH_v, are taken into account (because the experiments are, in general, performed at constant pressure, we use the enthalpy). Henceforth, the enthalpy is used with different dimensions, as convenient. The conversion of the enthalpy per *atom* is $\Delta H^\mathrm{a} \equiv \Delta H(\mathrm{J/atom}) = \Delta H(\mathrm{J/mol})/L = \Delta H(\mathrm{J/cm^3}) \times M/(\varrho L) = \Delta H(\mathrm{J/g}) \times M/L$ where L is the Avogadro number and M the atomic weight per mol. Values of ΔH_m and ΔH_v are listed in Table IV. The table shows that the latent heat of evaporation is, typically, 2−4 eV/atom (50–100 kcal/mol), while the latent heat of melting is, typically, 0.1−0.5 eV/atom (2–10 kcal/mol).

If phase changes take place, $U(\boldsymbol{x}, t)$ in (2.2.3) is non-zero and given by

$$U(\boldsymbol{x}, t)\,\mathrm{d}V \approx \boldsymbol{v}_{ls}\Delta H_\mathrm{m}\,\mathrm{d}F_{ls} + \boldsymbol{v}_{\mathrm{v}l}\Delta H_\mathrm{v}\,\mathrm{d}F_{\mathrm{v}l} \; , \tag{2.2.12}$$

where $\boldsymbol{v}_{ls}(\boldsymbol{x}, t)$, $\boldsymbol{v}_{\mathrm{v}l}(\boldsymbol{x}, t)$ and $\mathrm{d}F_{ls}$, $\mathrm{d}F_{\mathrm{v}l}$ are the respective velocities and surface elements of the liquid–solid and vapor–liquid interface within the volume element $\mathrm{d}V$. It is often convenient to introduce the *total* enthalpy, which can be approximated by

$$\Delta H(T) \approx \int_{T(\infty)}^{T} \varrho(T')c_\mathrm{p}(T')\,\mathrm{d}T' + \mathscr{H}(T - T_\mathrm{m})\Delta H_\mathrm{m} + \mathscr{H}(T - T_\mathrm{b})\Delta H_\mathrm{v}\ . \tag{2.2.13}$$

Here, the kinetic energy of the vapor is ignored. The first term describes the enthalpy density (J/cm^3; with solids and liquids this is equal to the energy density) required to heat the material from the temperature $T(\infty)$ to T. Note that in the case of vaporization this term includes the enthalpy change within the solid, liquid, and gas phases. The latter can be approximated, for an ideal gas, by $\Delta H_\mathrm{G} = \gamma R_\mathrm{G}\varrho_\mathrm{v}\Delta T/M(\gamma - 1)$, where $\gamma = c_\mathrm{p}/c_\mathrm{v}$ is the adiabatic index.

The second term describes the additional energy density necessary for melting. $\mathscr{H}$ is the Heaviside function, which is zero if $T < T_\mathrm{m}$ and unity if $T > T_\mathrm{m}$. The third term describes the latent heat of evaporation at the boiling temperature, T_b. Note, however, that vaporization may take place at temperatures $T_\mathrm{v} \lesssim T_\mathrm{b}$ (Chap. 11).

If we consider the liquid–solid system only and ignore density changes and also convective fluxes, the heat equation can be written together with (2.2.13) in the form

$$\frac{\partial \Delta H(\boldsymbol{x}, t)}{\partial t} - \nabla[\kappa(T)\nabla T(\boldsymbol{x}, t)] + \boldsymbol{v}_\mathrm{s}\nabla\Delta H(\boldsymbol{x}, t) = -\hat{\boldsymbol{k}}_\ell \nabla I(\boldsymbol{x}, t)\ , \tag{2.2.14}$$

where $\boldsymbol{v}_\mathrm{s}$ is the substrate velocity with respect to the laser beam. Equation (2.2.14) is most conveniently used with problems where latent heat effects play an important role (for a more general discussion see *Landau* and *Lifshitz*: Fluid Mechanics 1974). The situation is analogous with exothermal or endothermal chemical reactions when the energy of formation, ΔH, cannot be ignored with respect to the absorbed laser-light energy. In general, (2.2.14) can be solved only numerically [*Fell* et al. 2008].

2.2.5 Limits of Validity

The heat equation describes temperature distributions in many cases of thermal laser processing quite well. Nevertheless, one should be aware of the restrictions and uncertainties of calculated temperature distributions:

- The heat equation gives a macroscopic description of the medium averaged over a volume where thermal fluctuations are small. To estimate the length scale where such a description is appropriate, we consider a cube of side length l with N atoms (molecules) per unit volume. Then, the relative temperature fluctuation is $\delta T/T \approx (Nl^3)^{-1/2}$ and thus $l \approx (\delta T/T)^{-2/3}N^{-1/3}$. For $\delta T/T = 10^{-3}$ this yields $l \approx 0.02\,\mu\mathrm{m}$ for solids ($N \approx 10^{23}$ atoms/cm^3) and $l \approx 1\,\mu\mathrm{m}$ for gases with $N = 10^{18}$ atoms/cm^3. Thus, with submicrometer structures and with gases at low pressures, the application of the heat equation becomes inappropriate (Sect. 9.5.4).
- The values of α, R, κ, D, etc., are usually derived from static or quasi-static measurements where only small temperature gradients are involved. In laser

processing, however, the temperature gradients may be very strong and the interaction times very short. The temperature gradients are, typically, of the order $\nabla T \approx \Delta T/l$. Here, l is a characteristic length, for example, the radius of the laser focus, w, the heat diffusion length, l_{T}, the optical penetration depth, l_α, etc., depending on the particular problem. In any case, ∇T may be $10^5 - 10^{10}$ K/cm. As a consequence, the parameter values relevant in photothermal processing may significantly differ from those in conventional heat conduction problems.

- The optical properties of a specific medium depend on the laser parameters, which, in turn, affect the thermophysical properties via their temperature dependences. These dependences are often known in small temperature intervals only.
- The optical and thermal properties of a solid also depend on its surface morphology and crystallinity (amorphous, ceramic, poly- or single-crystalline), on surface contaminations (adsorbates, oxide layers, etc.), on defects (both physical defects such as dislocations, cracks, etc., and chemical defects such as isolated impurities, aggregate centers, etc.).
- The optical and thermal properties of liquids and gases depend on admixtures; with gases they also depend on pressure.
- Changes in parameter values originating from laser-induced changes in material properties introduce additional complications. Let us consider laser-CVD (Fig. 1.2.2a). Before nucleation takes place, α, R, D, κ, and the total emissivity, ε_{t}, are determined by the physical properties of the substrate material. When deposition commences, these quantities will rapidly change with the density and size of nuclei, and therefore with time. When a compact film is formed, e.g., a metal film, and when the penetration depth of the laser light is small compared to the film thickness, α, R, and ε_{t} will refer only to this deposited film. Similarly, D and κ will be quite different for such a combined structure compared to a uniform plane substrate. The situation is very similar in laser-induced surface modification and compound formation. Further complications arise if changes in surface geometry become significant. This is sometimes the case in materials deposition, etching, and ablation.
- The coupling between different degrees of freedom (e.g., the temperature, the density of species, N_i, etc.) causes feedbacks in the laser–matter interactions. Thus, from a theoretical point of view, a proper description of laser processing would require, in many cases, consideration of coupled non-linear equations.
- Whenever Knudsen effects are important, the kinetic Boltzmann equation instead of the heat equation should be solved. In reality, it is often possible to solve the problem for the Knudsen layer separately and derive modified boundary conditions for the heat equation.
- With ultrashort pulses where $\tau_\ell \leq D/v_0^2$ (v_0 is the sound velocity), the finite velocity of the heat front must be taken into account. Thus, the term $v_0^{-2}\partial^2 T/\partial t^2$ should be added to $D^{-1}\partial T/\partial t$ in the heat equation. This will result in a significant increase in temperature because the energy cannot be removed sufficiently fast enough from the heated volume (see, e.g., [*Vedavarz* et al. 1994]).

- With ultrashort pulses, the electrons and phonons are *not* in thermal equilibrium and 'hot' electron diffusion becomes important. In such cases one has to employ the 'two-temperature' model (Sect. 13.5).

In spite of these difficulties and restrictions, we will demonstrate in later chapters that essential features observed in laser processing can be understood from model calculations. In inhomogeneous media the propagation of light and heat must be calculated in a different way (Chap. 9).

In any case, the knowledge of laser-induced temperature distributions is a prerequisite for the modelling of processing rates, the clarification of the chemical kinetics, and the enlightenment of the basic microscopic interaction mechanisms. It is evident that it is desirable to measure as many of the relevant quantities as possible in situ, i.e., during laser processing.

2.3 Selective Excitations of Molecules

Laser photochemistry near or at molecule–solid interfaces can be based on selective electronic excitations of both the molecules and the solid surface, on selective vibrational excitations of the molecules, or on a combination of them. The excitation energy can also be transferred indirectly via an intermediate species as in photosensitization.

Electronic transitions of molecules are located mainly in the UV and VIS. Vibrational transitions are located in the IR. Both electronic transitions and vibrational transitions can be excited by single-photon (linear) processes or by multiphoton (MP) non-linear processes.

Laser-photochemical (non-thermal) processing is frequently based on *electronically* excited molecules and photofragments of them. There are, however, very few examples where selective single- or multiphoton *vibrational* excitations are of importance.

Different fundamental mechanisms involved in selective optical excitations of molecules and, to some extent, of solids have been studied for model systems. However, apart from a very few exceptions, only little is known about the photochemistry of systems relevant to LCP. Here, the physical conditions are very complex compared to the conditions in model systems.

The degree of selectivity achieved in a particular photoexcitation process is determined by the ratio of the excitation rate, W_{exc}, and the relaxation rate, W_{relax}. The selectivity is more pronounced the better the condition

$$W_{\mathrm{exc}} > W_{\mathrm{relax}} \tag{2.3.1}$$

is fulfilled. We shall term an excitation as selective if the system is *not* in local equilibrium. This shall include cases where the laser light induces a local temperature rise but without complete thermalization, e.g., between vibrational and translational degrees of freedom. In a mixture, selectivity can also denote the excitation of a

particular kind of species. The term non-selective or thermal excitation is used if the absorbed light energy is, at least locally, thermalized between the different degrees of freedom *and* the different kinds of species.

Subsequently, we shall summarize some basic aspects of selective electronic excitations and IR vibrational excitations.

2.3.1 Electronic Excitations

Electronic excitations of molecules can be based on single-photon or multi-photon processes. They are, in general, accompanied by simultaneous changes in the vibrational and rotational energy of the molecule.

Single-Photon Excitations

Let us consider some characteristic cases of single-photon (linear) excitations. Figure 2.3.1 shows potential energy curves for the electronic ground state and excited states of different molecules. According to the Franck–Condon principle, transitions occur vertically between maxima in the densities $|\psi_1|^2$ and $|\psi_2|^2$, where ψ_i are vibrational wave functions for the lower and upper electronic states. If the excited electronic state is unstable (Fig. 2.3.1a), excitation results in direct dissociation within times of, typically, 10^{-14} to 10^{-13} s. Clearly, relaxation and energy transfer between gas-phase molecules is unlikely within such short times. If the excited electronic state is stable, dissociation only occurs for photon energies $h\nu \geq E'_{\mathrm{D}}$ (Fig. 2.3.1b). However, in many cases dissociation of isolated molecules is even observed for $h\nu \leq E'_{\mathrm{D}}$ (Fig. 2.3.1c, d). This phenomenon is termed spontaneous predissociation. It is related to transitions from the initially excited electronic state to an unstable state (Fig. 2.3.1c) or to a stable electronic state whose dissociation energy is below the originally excited state (Fig. 2.3.1d). The final state can also be the electronic ground state itself; then, the molecule dissociates if $h\nu \geq E_{\mathrm{D}}$. Such intramolecular radiationless transitions result from the mixing of states near crossings of potential curves. They are therefore more common in polyatomic molecules than in diatomic molecules. The typical times for predissociation are between 10^{-12} and 10^{-6} s. Radiationless transitions are also termed internal conversion and intersystem crossing [*Avouris* et al. 1977; *Bixon* and *Jortner* 1968] or as Landau–Zener transitions [*Levine* and *Bernstein* 1987].

The main limitation of single-photon excitation/dissociation processes relevant to laser-chemical processing is the lack of flexibility of available lasers to match the maxima of dissociative transitions in the medium to far UV.

Densities of Excited and Dissociated Species

In photochemical laser processing, reaction rates are directly related to the average number of excited or dissociated molecules. Let us consider the problem for the simple photochemical process

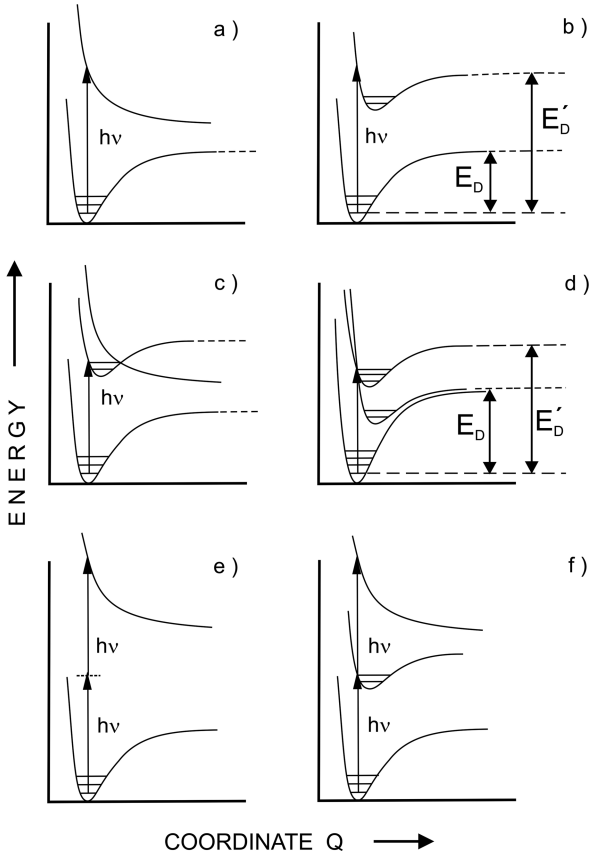

Fig. 2.3.1 a–f Potential energy curves for the electronic ground state and excited states of molecules, showing different cases of optical excitation and dissociation. E_{D} and E'_{D} are dissociation energies. Vibrational energy levels are only indicated. Rotational levels are not shown at all. Cases (**a**) to (**d**) show single-photon excitations. (**e**) Coherent two-photon excitation. (**f**) Sequential two-photon excitation. The energies of photons in cases (**e**) and (**f**) are not necessarily equal

$$\mathrm{AB}_{\mu} + h\nu \underset{\tau_{\mathrm{em}}}{\overset{\sigma}{\longleftrightarrow}} \mathrm{AB}^{*}_{\mu} \underset{\tau'_{\mathrm{rec}}}{\overset{\tau_{\mathrm{d}}}{\longleftrightarrow}} A + \mu B\,. \qquad \underset{\tau_{\mathrm{rec}}}{\longleftarrow} \tag{2.3.2}$$

The excitation of molecules AB_{μ} is characterized by the effective cross section, σ, at the particular laser wavelength. σ depends on the type of reactant, the gas pressure, etc. The effect of pressure broadening, line shifts, etc., also depends on the bandwidth of the laser light. The situation is similar for species AB_{μ} dissolved in a liquid. The effective cross section can significantly differ from the excitation (absorption) cross section for a single *isolated* molecule, σ_{a}. The latter is measured under collisionless conditions, and it has large values only if the photon energy

matches the distance between respective energy levels of the molecule and if the transition is allowed by symmetry (selection rules), i.e., if it is optically active. For $h\nu \geq E'_{\mathrm{D}}$ and negligible fluorescence, the absorption cross section is equal to the dissociation cross section, σ_{d}.

The relaxation time for deactivation of AB^*_μ is denoted by τ_{em}. τ_{d} describes the time for dissociation of AB^*_μ in a first-order decomposition process (Chap. 3). τ_{rec} and τ'_{rec} characterize the recombination of A and B to AB_μ and AB^*_μ, respectively. The relaxation times depend on gas pressure.

Electronic absorption and dissociation cross sections of molecules that are of particular relevance in laser processing are summarized in Table V for different laser wavelengths. Most of the values of σ found in the literature refer to effective cross sections.

For an estimation of photochemical processing rates, the concentrations of species A and AB^*_μ, x_{A} and x_{AB^*}, must be known. Stationary values of these are given in [*Bäuerle* 1996].

Multiphoton Excitations

Multiphoton (MP) processes open up additional excitation/dissociation channels and thereby permit one to use the laser light at a particular wavelength more efficiently or to use a much wider variety of precursor molecules.

The number of molecules excited in a MP process depends non-linearly on photon flux. Figures 2.3.1e, f show two different kinds of MP excitations. If the photon energy is smaller than the energy difference between the first optically active excited state and the ground state, excitation is possible only via *coherent* two-photon absorption (case e). The absorption cross section for coherent n-photon excitations is henceforth denoted by ${}^{(n)}\sigma$. The situation is different in case f. Here, the molecule is transferred to the first excited state by absorption of a single photon. The absorption of an additional photon results in dissociation. This process is denoted as *sequential* two-photon absorption. In the simplest case, the cross section of a sequential n-photon excitation is proportional to $\prod_i^n {}^{(1)}\sigma_i$, where ${}^{(1)}\sigma_i$ is the single-photon absorption cross section; $\prod$ denotes the product. The energies of the single photons involved in a MP process are not necessarily equal.

Efficient MP processing can only be performed with high-power pulsed lasers. Because such laser pulses may cause substrate damage, most applications of MP processing are performed with an irradiation geometry where the laser beam propagates parallel to the substrate surface (Fig. 1.2.2b). The relevant processing step can be based on MP ionization (MPI), MP dissociation (MPD), or MP excitation of the precursor molecules.

Photosensitization

Photosensitization denotes a process where photons are absorbed by intermediate species which transfer their excitation energy to acceptor molecules via

collisions [*Calvert* and *Pitts* 1966]. For example, direct photolysis of CH_4 is only possible below 144 nm,

$$CH_4 + h\nu(\lambda < 144\,\text{nm}) \rightarrow CH_2 + H_2\,, \tag{2.3.3}$$

while the Hg-photosensitized reaction can take place at a longer wavelength,

$$Hg(^1S_0) + h\nu(\lambda = 253.7\,\text{nm}) \rightarrow Hg(^3P_1) \tag{2.3.4}$$

$$Hg(^3P_1) + CH_4 \rightarrow Hg(^1S_0) + CH_3 + H\,. \tag{2.3.5}$$

As can be seen from this example, the photoproducts are not necessarily the same in both cases.

Photosensitized reactions are very common in photochemical studies, but cannot be employed in laser microchemistry due to the delocation of the reaction in this process. However, the technique has been applied for large-area, low-temperature growth of epitaxial layers of HgTe [*Irvine* et al. 1984], the deposition of hydrogenated amorphous silicon (a-Si : H) [*Kamimura* and *Hirose* 1986], and etching reactions [*Loper* and *Tabat* 1984].

2.3.2 Infrared Vibrational Excitations

In this subsection we shall discuss some fundamentals on vibrational excitations of free molecules in the electronic ground state. Special emphasis is put on aspects that are relevant to LCP.

Excitation of Isolated Diatomic Molecules

Vibrational excitation of single *isolated* molecules can be realized within the collisionless environment of a molecular beam. Figure 2.3.2 shows an anharmonic potential which shall represent the electronic ground state. Because of anharmonicity, the vibrational levels are not equally spaced. Rotational levels are ignored in the figure although they are essential in excitation processes. For simplicity, we always use the term vibrational transition, even when the rotational state of the molecule is changed simultaneously.

The simplest absorption process is a one-photon (linear) excitation of the vibrational state, $v = 1$, as shown by arrow a. The excitation energy $h\nu = E_{v=1} - E_{v=0}$ is, typically, between $100\,\text{cm}^{-1}$ and some $1000\,\text{cm}^{-1}$ (about 0.01 eV to some 0.1 eV). Arrows b and c indicate excitations of the third and fourth vibrational level by *coherent* two- and three-photon processes, respectively. Such MP processes become quite unlikely for excitations $v > 4$, because of the rapid decrease in σ with such highly non-linear processes. Vibrational levels $v = 2, 3, \ldots$ can also be excited, although with low probability, in a one-photon overtone absorption process using a photon energy $h\nu' = E_v - E_{v=0}$. This is indicated for $v = 2$ by arrow d. MP absorption by *sequential* excitation (case e) becomes quite unlikely for high vibrational levels as

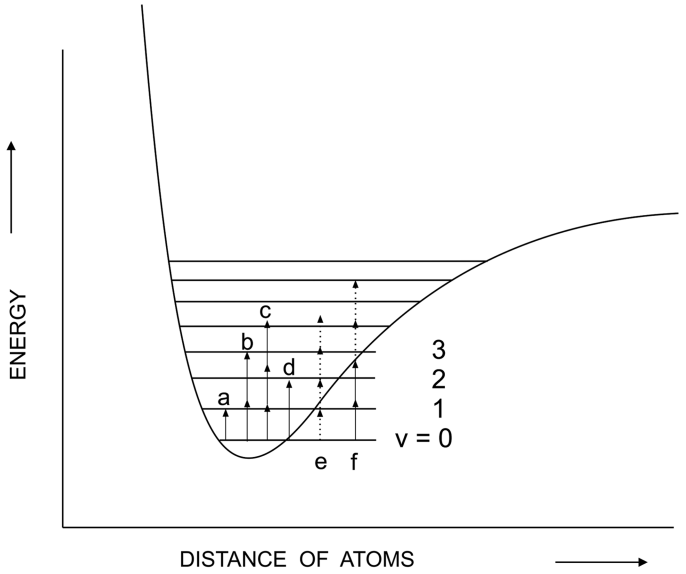

Fig. 2.3.2 Various types of IR vibrational excitations of a single isolated diatomic molecule. For simplicity, rotational levels have been ignored, **a**: one-photon excitation; **b, c**: coherent two- and three-photon excitation; **d**: one-photon overtone excitation; **e**: sequential four-photon excitation; **f**: two-photon coherent excitation (*solid arrows*) followed by sequential excitation (*dotted arrows*). The energies of photons employed in multiphoton excitation processes are not necessarily equal

well, simply because of the (increasing) mismatch between the photon energy and the vibrational energy levels. A combined excitation process is shown in case f. Here, two-photon coherent absorption (solid arrows) is followed by two-photon sequential absorption (dotted arrows). In this way, higher vibrational levels can be excited.

Excitation of Isolated Polyatomic Molecules

In contrast to diatomic molecules, polyatomic molecules can absorb a great number of monochromatic photons even under collisionless conditions. This can be seen from Fig. 2.3.3. The 'superposition' of different vibrational-level systems, corresponding to different normal modes of the molecule, results in different regions of vibrational-level densities. At low energies the vibrational levels are discrete. With increasing energy, their density increases rapidly. The region above a certain energy, E_s, is denoted as *quasi-continuum*. E_s corresponds to, typically, three to ten vibrational quanta for simple polyatomic molecules and to only one vibrational quantum for molecules consisting of many atoms, or such with heavy atoms.

Selective excitation of the particular mode that is in resonance with the IR laser frequency takes place as discussed with diatomic molecules. If this resonant mode is excited up to the quasi-continuum, even a weak intermode anharmonicity is

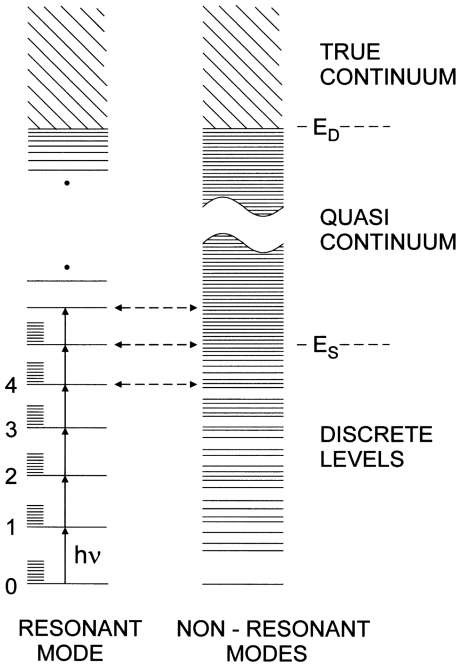

Fig. 2.3.3 Multiphoton vibrational excitation and dissociation of a polyatomic molecule by intense IR radiation. *Left*: vibrational-rotational levels for the mode that is selectively excited by the IR radiation. *Right*: three regimes of vibrational level densities: discrete levels of non-resonant modes, vibrational quasi-continuum, and true continuum

sufficient to cause stochastization of the vibrational energy. In other words, when the vibrational energy stored in the selectively driven mode approaches E_s, it will spread over all the different modes. This mechanism diminishes the number of vibrational quanta in the resonant mode and thereby permits further laser-light absorption. This process takes place again and again. Thus, the vibrational degrees of freedom are subjected to strong heating. The true continuum is reached at the dissociation energy, E_D. Dissociation of the vibrationally excited molecule will take place, in general, via the *lowest* dissociation channel. With the high excitation rates that can be achieved with intense IR lasers, many-photon *superexcitation* of polyatomic molecules far above the dissociation energy has been observed.

The rate of vibrational excitation of a single polyatomic molecule is often written as

$$W_{ex} = \sigma \frac{I}{h\nu}\,, \tag{2.3.6}$$

where σ is the *average* absorption cross section, which depends on laser fluence and pulse length. For polyatomic molecules, σ has values of, typically, 10^{-20} to $10^{-18}\,\mathrm{cm}^2$. The average number of IR photons absorbed per pulse by a *single*

molecule is $\langle n \rangle = \sigma\phi/h\nu$. With polyatomic molecules, 10–100 IR photons can be absorbed with fluences $\phi \approx 1-10\,\mathrm{J/cm^2}$.

Collisionless IR-MP excitation and dissociation of many molecules which are used as precursors in laser-chemical processing, such as SF_6, BCl_3, $CO(CF_3)_2$, CF_3I, and CDF_3, is consistent with the model in Fig. 2.3.3. Highly vibrationally excited molecules and radicals produced by IR-MP excitation/dissociation interact with solid surfaces quite differently than molecules in the vibrational ground state. Examples will be given in various chapters.

The Role of Collisions

Collisions will not only change the lifetime of a particular excitation, but also permit high-level vibrational excitation and dissociation of even diatomic molecules via near-resonant energy transfer. For *pure* gaseous CO, this process can be described by

$$\begin{aligned} \mathrm{CO}(v=0) + h\nu &\leftrightarrow \mathrm{CO}(v=1) \\ \mathrm{CO}(v=1) + \mathrm{CO}(v=1) &\leftrightarrow \mathrm{CO}(v=2) + \mathrm{CO}(v=0) \\ \mathrm{CO}(v=2) + \mathrm{CO}(v=1) &\leftrightarrow \mathrm{CO}(v=3) + \mathrm{CO}(v=0) \end{aligned} \qquad (2.3.7)$$

etc. The transition $v = 0 \rightarrow 1$ which is in resonance with the photon energy $h\nu$ is excited in a one-photon process (Fig. 2.3.2). Subsequently, the energy is transferred to other excited molecules. Thereby, high vibrational states, up to the dissociation limit, can be reached. The same process can take place with lower efficiency (unless there is a coincidence in vibrational energies), between *different* molecules, A and B, including isotopes.

Selectivity

The selectivity of a particular photo-excitation process is determined by (2.3.1). The redistribution of vibrational energy is determined by different relaxation times:

- The time required for spontaneous radiative (dipolar) transitions between low-lying, well-separated vibrational levels which determines the natural linewidth. This is, typically, of the order of 10^{-3} s.
- The time required for *intra*molecular transfer of vibrational energy between different vibrational modes being excited, $\tau_{\text{v-v}}^{\text{A}}$. This time decreases with increasing vibrational anharmonicity and increasing density of vibrational levels. Within the quasi-continuum it is, typically, of the order of 10^{-13} to 10^{-11} s.
- The time required for *inter*molecular transfer of vibrational energy via collisions between molecules either of the *same* kind, $\tau_{\text{v-v}}^{\text{A-A}}$, or of *different* kinds, $\tau_{\text{v-v}}^{\text{A-B}}$. For low-level excitations, energy exchange between molecules of different kinds is less efficient because of the mismatch of vibrational energy levels. For highly excited states the type of colliding molecules becomes almost unimportant.

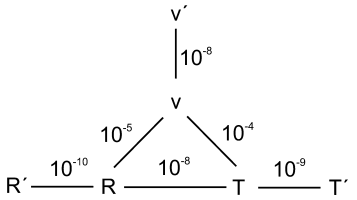

Fig. 2.3.4 Different relaxation channels for energy transfer during binary collisions of molecules, $v' - v$ stands for vibrational-vibrational, $v - T$ for vibrational-translational, and $R - T$ for rotational-translational processes. The numbers represent typical relaxation times for pure gases at 300 K in units of sbar [*Eyring* et al. 1980]

- The time required for molecular vibrational energy to be transferred to translational degrees of freedom, $\tau_{v\text{-}T}$. This is the time required to reach thermal equilibrium within the molecular mixture.

Clearly, $\tau_{v\text{-}v}^{A\text{-}A}$, $\tau_{v\text{-}v}^{A\text{-}B}$, and $\tau_{v\text{-}T}$ vary with experimental conditions such as the molecular density, temperature, and the type of admixtures or solvents. Figure 2.3.4 shows, schematically, various energy-transfer processes and the corresponding relaxation times that are typical for *binary collisions* of gas-phase molecules at 300 K and 1000 mbar. With these conditions, the time between successive collisions is $\tau_c \approx 10^{-10}$ s ($\tau_c^{-1} \approx N\langle\sigma_c v\rangle$; σ_c is the cross section for collisions and v the velocity of molecules).

Classification of IR-MP Photochemistry

IR-MP photochemistry based on pulsed-laser excitation of high vibrational states can be classified into four different cases:

Mode- or *bond-selective* photochemistry requires an excitation rate that is large compared to the rate of intramolecular vibrational energy transfer. This would need both a mode which is fairly isolated from other vibrational modes and high-intensity picosecond or femtosecond resonant excitation. Mode isolation is well fulfilled for diatomic molecules, because they have only one vibrational degree of freedom. In fact, vibrationally enhanced photochemical reactions based on low-level excitations of diatomic molecules have been reported. Collisionless MP, high-level excitation/dissociation by monochromatic infrared radiation is, however, unlikely/impossible (Fig. 2.3.2). For polyatomic molecules the situation is somewhat complementary. They permit high-level vibrational excitation but no bond selectivity (Fig. 2.3.3). Laser processing based on bond-selective vibrational excitation/dissociation of precursor molecules has not been demonstrated.

The (three) remaining cases of selective vibrational excitations have been employed in laser processing:

Molecule-selective excitation requires

$$W_{ex} \gg \frac{1}{\tau_{v\text{-}v}^{A\text{-}B}} . \tag{2.3.8}$$

The vibrational energy within molecules A which interact with the IR light is in equilibrium. Other molecules within the mixture, B, that are *not* directly excited are in lower vibrational states. Thus, molecules in resonance with the laser frequency acquire a higher vibrational temperature than all other molecules. High-level, molecule-selective vibrational excitation can take place as discussed with regard to Fig. 2.3.3, and via collisions analogous to (2.3.7). The time for energy transfer from A to B or from A to surface atoms, $\tau_{\text{v-v}}^{\text{A-B}}$, must be long compared to the time of resonant energy transfer, A to A.

Molecule-selective excitation and dissociation is of practical interest, e.g., in laser *isotope separation* [*Letokhov* 1983]. With isotopes whose mismatch between vibrational levels is of the order of $k_{\text{B}}T$, collisional excitations of the type (2.3.7) must be avoided.

Non-equilibrium excitation is achieved if

$$W_{\text{ex}} \gg \frac{1}{\tau_{\text{v-T}}} \,. \tag{2.3.9}$$

In this case, there may be vibrational equilibrium among all molecules in the mixture, but no equilibrium between vibrational and translational degrees of freedom. Condition (2.3.9) can only be fulfilled if the gas mixture does not contain any component with fast v − T relaxation. For example, with pure SF_6 one finds that with gas pressures $p(SF_6) \approx 0.1$ mbar and low cw CO_2-laser-light intensities, about 50% of the molecules can be in a non-equilibrium state. Because of the difference in the vibrational and translational temperatures, non-selective vibrational photochemistry is possible when the time constant for the *fastest* reaction channel is shorter than $\tau_{\text{v-T}}$. The most important application is IR laser-induced radical synthesis [*Letokhov* 1988].

Photothermal excitation is characterized by

$$W_{\text{ex}} \ll \frac{1}{\tau_{\text{v-T}}} \,. \tag{2.3.10}$$

All molecules within the reaction volume defined by the laser beam are in thermal equilibrium. The vibrational energy is immediately thermalized.

Since σ in (2.3.6) and $\tau_{\text{v–T}}$ depend on temperature, (2.3.9) transforms to

$$W_{\text{ex}}\tau_{\text{v–T}} = \sigma(T)\frac{I}{h\nu}\tau_{\text{v–T}}(T) \gg 1 \,. \tag{2.3.11}$$

The decrease in relaxation time with temperature can be described by the Landau–Teller relation, $\tau_{\text{v–T}}(T) = \tau_{\text{v–T}}(0)\exp(\mu/T^{1/3})$, where $\mu > 0$. The cross section $\sigma(T)$ can increase or decrease with temperature. Because $T = T(I)$, (2.3.11) is a non-monotonic function of intensity with regions that correspond to either thermal or non-thermal gas-phase excitations.

2.4 Surface Excitations

In this section we give an overview on non-thermal or not purely thermal excitations of solid surfaces and adsorbate–adsorbent systems.

2.4.1 External Photoeffect

The external photoeffect denotes the ejection of electrons from a solid surface that is irradiated with photons. With metals, photoelectron emission is observed if $h\nu \geq h\nu_G$, where ν_G denotes a threshold frequency which is located within the VIS and UV [λ_G(Cs, Cu, Pt) $\approx$ 639, 277, 231 nm]. Photoelectron emission has also been observed with semiconductors and insulators. With photon energies $h\nu < E_g$, such electrons may originate from single-photon excitations of occupied electron traps within the band gap or from MP excitations across E_g (Fig. 2.1.1). The latter mechanism seems to be quite common with ps- and fs-laser pulses. In any case, if the solid is immersed in a reactive ambient, molecules that capture an electron can become unstable. Spontaneous decay or partial fragmentation of the molecule may be the consequence [*Schröder* et al. 1987]. Further fragmentation can take place via collisions with other molecules or with the substrate surface (Fig. 2.4.1).

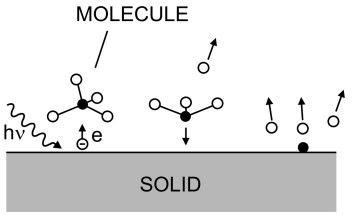

Fig. 2.4.1 Decomposition of a molecule by photoelectron capture

2.4.2 Internal Photoeffect

The internal photoeffect is the generation of electron–hole pairs in semiconductors or insulators by single-photon or multiphoton excitation (Fig. 2.1.1; we will not bother with direct and indirect processes as this is outlined in standard textbooks). Electrons and holes change the optical properties of the material and thereby its interaction with laser light (Sect. 7.6). Moreover, photocarriers play a fundamental role in many types of molecule–surface interactions relevant in LCVD, surface modification, and etching (Fig. 15.1.1). The analysis of such processes requires detailed information on the carrier distribution.

Carrier Densities

For an intrinsic semiconductor, the carrier density can be described, in a simple approximation, by

$$\frac{\partial N_c(\boldsymbol{x},t)}{\partial t} = \alpha(\nu)\frac{I(\boldsymbol{x},t)}{h\nu} - k^{rec}[N_c(\boldsymbol{x},t) - \overline{N}_c(T)] + \nabla[D_c(\boldsymbol{x},t)\nabla N_c(\boldsymbol{x},t)]\,. \tag{2.4.1}$$

The first term describes the generation of photocarriers by inter-band absorption. The second term represents the loss of carriers by recombination, where $k^{rec} = \tau_{rec}^{-1}$ is the rate constant for electron–hole pair recombination and $\overline{N}_c(T)$ the carrier density in (thermal) equilibrium. The last term describes the diffusion of carriers.

The recombination time, τ_{rec}, depends on the material and the concentration of photocarriers. It is determined by direct or indirect band-to-band recombination, by multicarrier (Auger) recombination, and by defects and impurities. Thus, values of τ_{rec} near the surface differ somewhat from those within the bulk. τ_{rec} is, typically, between a few picoseconds and several seconds.

The diffusion coefficient can be written as

$$D_c = \frac{\sigma_e D_e + \sigma_h D_h}{\sigma_e + \sigma_h}\,. \tag{2.4.2}$$

D_e and D_h are the actual diffusion coefficients of electrons and holes and σ_e and σ_h the corresponding conductivities.

Equation (2.4.1) ignores laser-induced heating and collective (plasma) phenomena which are observed at very high carrier densities [*Yoffa* 1980].

Let us consider electron–hole pair generation in some more detail for silicon. Because E_g (Si; 300 K) $\approx$ 1.1 eV, bandgap excitations become possible with $\lambda < 1\,\mu$m. With increasing temperature, E_g decreases, and thereby the minimum photon energy for excitation. With carrier densities $N_c > 10^{18}\,/\mathrm{cm}^3$, Auger recombination becomes dominant. Then, the carrier lifetime decreases with increasing concentration as

$$\tau_{rec} = \frac{1}{k^{rec}} \propto \frac{1}{N_c^2}\,. \tag{2.4.3}$$

For room temperature, the second term in (2.4.1) can be substituted by ζN_c^3 with $\zeta \approx 4 \times 10^{-31}\,\mathrm{cm}^6/\mathrm{s}$. For example, an initial carrier density of $N_c = 10^{22}\,/\mathrm{cm}^3$ decreases via Auger recombination within about 10^{-10} s to 1%.

Avalanche Ionization

With high laser-light intensities, the rate of electron excitation may overtake the rate of energy loss via generation of phonons. Then, electrons become highly excited and, eventually, attain sufficient energy to generate secondary electron–hole pairs by impact ionization of lattice atoms/molecules (the contribution of holes can often be ignored because of their low mobility, in particular in insulators and large bandgap semiconductors). Because of the positive feedback involved in this process, very high electron densities can be generated. This effect is often termed avalanche ionization. With such conditions, even originally highly transparent materials can become strongly absorbing and, as a consequence, *optical breakdown* and plasma formation is often observed.

With very high laser-light intensities, electrons may even be generated when $h\nu < E_g$. This is mediated via highly non-linear processes such as defect enhanced or coherent MP absorption (Fig. 2.1.1), light-induced defect formation, thermal ionization, and MP ionization (MPI). Further details on multiphoton- and avalanche-ionization are presented in Sect. 13.6.

2.4.3 Electromagnetic Field Enhancement, Catalytic Effects

Various types of electromagnetic field enhancements observed on solid surfaces can significantly alter both surface morphologies and reaction rates in laser-material processing [*Plech* et al. 2009; *Brodoceanu* et al. 2007; *Aussenegg* et al. 1983]. Such field enhancements may be related to surface roughnesses, nucleation centers, clusters, the excitation of surface polaritons or plasmons, interference phenomena, particulates etc. Further details are outlined in Sect. 5.3.7.

The physical and chemical properties of surfaces change during laser ablation, etching, deposition, doping, and surface modification. Changes in surface properties may cause autocatalytic effects, as observed during laser-induced metal deposition, catalyze electroless plating, as observed after polymer ablation, etc.

Some of these different effects are discussed in detail in other chapters.

2.4.4 Adsorbed Molecules

Adsorption of molecules on solid surfaces changes their electronic and vibrational properties and thereby the absorption cross section for the interaction with light. Additionally, the number of vibrational degrees of freedom can increase. With a diatomic molecule such as CO, adsorption changes the number of vibrational degrees of freedom from one to six (Fig. 2.4.2). *Selective* electronic or vibrational excitation of adsorbate–adsorbent systems may result in selective desorption or photolysis of adsorbed species, in changes in the catalytic properties of the surface, etc. [*Aussenegg* et al. 1983].

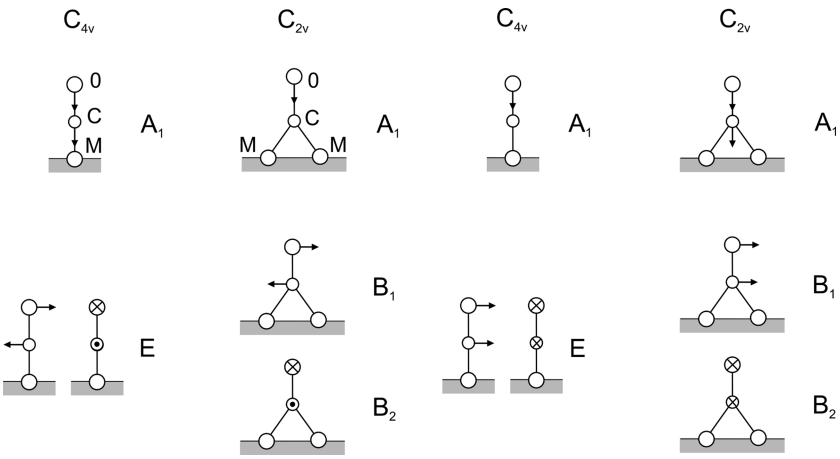

Fig. 2.4.2 Normal modes of CO molecules adsorbed on a metal surface in top site (C_{4v} symmetry) and bridging site (C_{2v} symmetry) positions; ⊗ and ⊙ indicate elongations perpendicular to the plane of the drawing. Vibrations with A and B symmetry are non-degenerate, vibrations with E symmetry are two-fold degenerate

It should be emphasized that the consideration of *single* effects oversimplifies the situation. A real understanding of chemical reactions at interfaces requires simultaneous treatment of the different interactions in the gas phase, adsorbed phase, and solid phase and, in addition, the often subtle couplings between them.

http://www.springer.com/978-3-642-17612-8

Laser Processing and Chemistry
Bäuerle, D.W.
2011, XXII, 851 p., Hardcover
ISBN: 978-3-642-17612-8